STATENS GEOTEKNISKA INSTITUT

SWEDISH GEOTECHNICAL INSTITUTE

No. 10

SÄRTRYCK OCH PRELIMINÄRA RAPPORTER

REPRINTS AND PRELIMINARY REPORTS

Supplement to the ''Proceedings'' and ''Meddelanden'' of the Institute

Triaxial Tests on Thin-Walled Tubular Samples

1. Effects of Rotation of the Principal Stress Axes and of the Intermediate Principal Stress on the Shear Strength

   by B. B. Broms and A. O. Casbarian

2. Analysis of the Triaxial Test - Cohesionless Soils

   by B. B. Broms and A. K. Jamal

Reprinted from the Proceedings of the Sixth International Conference on Soil Mechanics and Foundation Engineering, Montreal 1965. Vol. 1.

STOCKHOLM 1965

Preface

The investigations reported in this publication, and resulting in two papers, were carried out at Cornell University under the guidance of the senior author. Since then the author has accepted a position as director of the Swedish Geotechnical Institute. The Institute has therefore decided to include the papers in its series Reprint and Preliminary Reports.

Stockholm, December, 1965

SWEDISH GEOTECHNICAL INSTITUTE

Effects of Rotation of the Principal Stress Axes and of the Intermediate Principal Stress on the Shear Strength

Effets de la contrainte principale intermédiaire et de la rotation des axes des contraintes principales sur la résistance au cisaillement d'une argile remaniée

B. B. BROMS, PH.D., *Associate Professor, Cornell University, Ithaca, U.S.A.*
A. O. CASBARIAN, PH.D., *Shell Development Company, Houston, U.S.A.*

SUMMARY

Three series of consolidated-undrained triaxial tests were carried out on hollow cylindrical specimens of a remoulded kaolinite clay. In series I and II the effects of rotation of the principal stress axes and of the intermediate principal stress were investigated separately. The combined effects were investigated in series III. Series I and II indicated that both the rotation of the principal stress axes and the intermediate principal stress have an appreciable effect on the deviator stress, the friction angle ϕ', and the pore-pressure coefficient A_f. Series III indicated that the shear-strength and pore-pressure parameters of a soil can be predicted for any rotation of the principal stress axes and for any value of the intermediate principal stress by the principle of superposition.

SOMMAIRE

Trois séries d'essais triaxiaux non-drainés ont été faites sur des échantillons creux et cylindriques de kaolin remoulé. Dans les séries I et II les effets de rotation des axes des contraintes principales et les effets de la contrainte principale intermédiaire ont été examinés. Ces effets combinés furent examinés dans la série III. Les séries I and II indiquent que la rotation des axes des contraintes principales et que la contrainte principale intermédiaire ont un effet sensible sur la déviateur $(\sigma_1 - \sigma_3)$, 1' angle ϕ' et la pression interstitielle. La série III indique que les caractéristiques de la résistance d'un sol peuvent être prédites pour chaque rotation des axes des contraintes principales et pour chaque valeur de la contrainte principale intermédiaire par le principe de superposition.

ROTATION OF THE PRINCIPAL STRESS AXES frequently takes place under field conditions such as during the construction of earth dams. This rotation may have an appreciable effect on the shear-strength and pore-pressure parameters of a soil and hence may affect appreciably the design of such structures. Failure of many types of foundation structures, such as sheet pile walls and long footings, as well as slope failures of cuts and fills frequently takes place under the condition of plane strain. No lateral movements take place along the axes of these structures and the principal stress which acts in the direction of the axis of these structures will attain a value intermediate between the major and minor principal stresses.

The effects of the intermediate principal stress on the shear-strength and pore-pressure parameters of cohesive soils have been studied by Rendulic (1936), Habib (1953), Taylor (1955), Henkel (1958), Hirschfeld (1958), and Wu, Loh, and Malvern (1962) by means of compression and extension tests. However, the results reported by these investigators are conflicting. This paper presents the results of an investigation concerned with the effects of the rotation of the principal stress axes and of the intermediate principal stress on the shear-strength and pore-pressure parameters of a saturated remoulded kaolinite clay. Hollow cylindrical specimens were tested to failure under consolidated-undrained conditions at different rotations of the principal stress axes and at different values of the intermediate principal stress. The pore pressures developed during the undrained part of each test were measured.

EXPERIMENTAL PROGRAMME

Test Apparatus and Loading Unit

Hollow cylindrical test specimens were used in this investigation. The dimensions of the test specimen are shown in Fig. 1. The hollow clay cylinders were enclosed between an inner and an outer rubber membrane and were placed in a modified triaxial cell. Filter paper drains were placed along the outside and the inside perimeters to facilitate

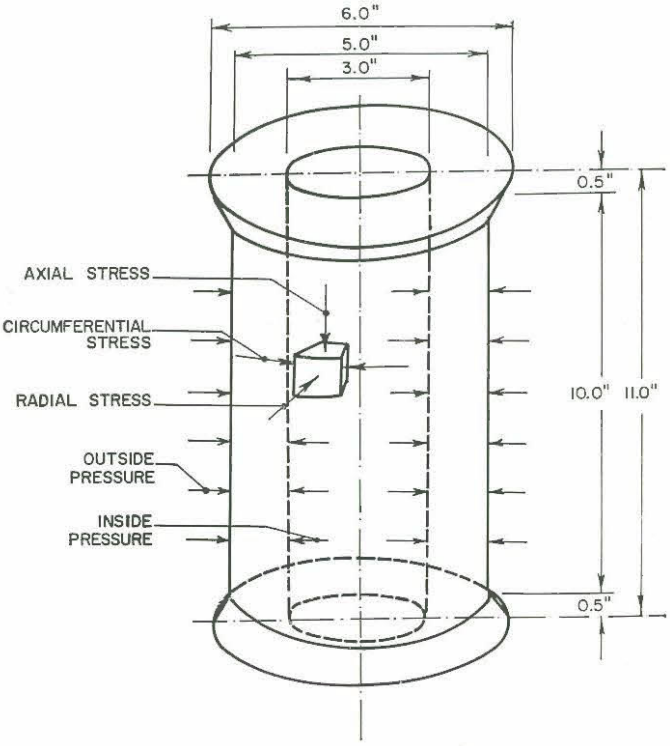

FIG. 1. Dimensions of test member.

Reprinted from *Proc. 6th internat. Conf. Soil Mech., 1965.* Printed in Canada.

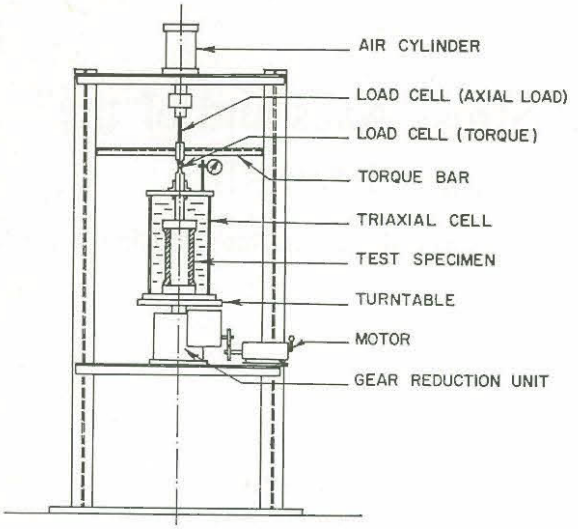

FIG. 2. Test arrangement.

drainage and to improve pore-pressure equalization. The pressures within the inside and outside chambers could be varied independently, as well as the axial load. The test specimens were loaded by the unit shown in Fig. 2. Axial load was applied by an air cylinder and kept constant by a sensitive air pressure regulator. Torque was applied by rotating the triaxial cell which was rigidly attached to a turntable. The applied axial load and the applied torque were measured by load cells to an accuracy of at least one per cent.

Stress Analysis

The inside and outside chamber pressures were chosen so that the average radial stress (Fig. 1) was equal to the intermediate principal stress σ_2 and that the major and minor principal stress axes were contained in the plane of the axial and circumferential stresses. The major and minor principal stresses (σ_1 and σ_3, respectively) have been calculated from the average axial stress, the average circumferential stress, and the average shear stress. Stress analyses based on theory of elasticity and theory of plasticity have indicated that the difference between the average stress and that determined from a more accurate analysis is small (Casbarian, 1964).

The torque measurements were corrected for the restraining effects caused by the ruhber membranes, the filter paper drains, and the friction between the piston and the bushing of the triaxial cell. Similar corrections were not made for the axial load.

Material

A kaolinite clay of medium plasticity and of medium dry strength was used. Some of its index properties are as follows: liquid limit = 57 per cent; plastic limit = 32 per cent; clay fraction (< 0.002 mm) = 39 per cent; specific gravity = 2.68; coefficient of consolidation = 7.9×10^{-3} sq.cm./sec; and coefficient of permeability = 1.97×10^{-4} cm/sec.

Preparation of the Soil

The clay, which was obtained in powder form, was mixed in ten batches at a water content of 48.5 per cent. Each batch was stored separately in a humid room for at least four weeks before testing and each batch was sufficient to form at least five test specimens. The hollow specimens were fabricated by compacting the remoulded clay with a tamper between an inner and an outer mould. Special care was taken to eliminate all voids.

Test Procedure

After moulding, the test specimens were consolidated isotropically at a confining pressure of 7.0, 25.0, or 70.0 lb/sq.in. The time required for 90 per cent consolidation was approximately 20 minutes. However, the test specimens were allowed to consolidate for at least eight hours. At the end of the consolidation phase, de-aired water was circulated through the porous stones and through the pore-pressure lines to remove any trapped air. During the undrained phase of the consolidated-undrained tests a back pressure of 20 lb/sq.in. was used to ensure full saturation. All tests were stress controlled except for those in which rotation of the principal stress axes occurred. These tests were strain controlled. The loading rate was adjusted to allow at least 95 per cent equalization of pore pressures during all phases of the test programme. Approximately eight hours were required for the undrained part of each test.

The effects of the rotation of the principal stress axes on the shear-strength and pore-pressure parameters were investigated in series I. The soil samples, which were initially isotropically consolidated, were tested to failure under undrained conditions. During the undrained phase the intermediate principal stress and the radial stress were maintained constant at a value equal to the consolidation pressure. Both compression and extension tests were carried out. For the compression tests the axial stress was increased and the circumferential stress was decreased by the same amount. For the extension tests the circumferential stress was increased while the axial stress was decreased. For tests in which rotation occurred, the samples were thereafter tested to failure through the application of torque.

The rotation of the principal stress axes has been expressed by the angle α. This angle is equal to the rotation of the major principal stress axis which takes place during the undrained phase. A positive value of the angle α indicates a compression test while a negative value indicates an extension test.

In series II the effects of the intermediate principal stress were investigated. No rotation of the principal stress axes was allowed. During the undrained phase the intermediate principal stress (equal to the average radial stress) was kept constant at a value equal to the consolidation pressure. The major and minor principal stresses, σ_1 and σ_3, respectively, were adjusted in such a way that at failure the ratio N, equal to $(\sigma_2 - \sigma_3)/(\sigma_1 - \sigma_3)$, varied between 0 and 1.0. A value of $N = 0$ corresponds to the standard compression test. For this test the intermediate principal stress σ_2 was equal to the minor principal stress.

In series III the combined effects of rotation of the principal stress axes and of the intermediate principal stress were investigated. Both compression and extension tests were carried out. In this series the direction of the major principal stress axis rotated between 0° and ± 45° and the ratio N varied between 0 and 1.0. During the undrained phase, the test samples were subjected initially to an increase or decrease of the axial stress. Thereafter, for the tests in which rotation occurred, the samples were loaded to failure by applying a torque.

TEST RESULTS

Series I

The test results from series I are tabulated in Table I. The relationships between the pore-pressure coefficient A_f,

TABLE I. TEST RESULTS

Test no.	Consolidation pressure, p_c (lb/sq. in.)	Rotation of stress axes α (deg.)	Stress ratio N	Pore-pressure coefficient, A_f	Deviator stress $(\sigma_1 - \sigma_3)_{max}$ (lb/sq. in.)	Friction angle, ϕ' (deg.)
			Series I			
A(1)	7.0	0	0.5	0.74	8.2	
A(2)		19	0.5	0.69	7.9	
A(3)		30	0.5	0.81	6.5	
A(4)		45	0.5	0.84	6.2	
A(5)		61	0.5	0.82	6.8	
A(6)		70	0.5	0.81	8.5	
A(7)		90	0.5	0.79	7.8	
B(1)	25.0	0	0.5	0.76	25.6	
B(2)		23	0.5	0.80	23.0	
B(3)		32.5	0.5	0.85	19.0	
B(4)		45	0.5	0.91	20.0	
B(5)		57	0.5	0.90	19.2	
B(6)		71	0.5	0.88	20.3	
B(7)		90	0.5	0.80	24.0	
C(1)	70.0	0	0.5	0.82	62.0	35.7
C(2)		17	0.5	0.89	54.6	32.0
C(3)		29.5	0.5	0.99	48.0	29.9
C(4)		45	0.5	1.11	41.0	28.2
C(5)		61	0.5	1.05	46.2	29.9
C(6)		73	0.5	0.98	52.8	32.0
C(7)		90	0.5	0.84	61.4	35.7
			Series II			
A(21)	7.0	0	0.00	0.42	8.10	
A(22)		0	0.25	0.52	7.87	
A(1)or(7)		0	0.50	0.74	8.20	
A(24)		0	0.73	0.85	7.70	
A(25)		0	1.00	1.04	6.70	
B(21)	25.0	0	0.00	0.53	24.6	
B(22)		0	0.21	0.59	28.4	
B(1)or(7)		0	0.50	0.80	24.0	
B(24)		0	0.74	0.94	22.8	
B(25)		0	1.00	1.14	18.5	
C(21)	70.0	0	0.00	0.67	60.0	29.2
C(22)		0	0.25	0.77	63.0	34.4
C(1)or(7)		0	0.50	0.84	61.4	35.7
C(24)		0	0.70	0.97	50.0	35.9
C(25)		0	1.00	1.17	47.5	36.0
			Series III			
A(21)	7.0	0	0.00	0.42	8.1	
A(32)		29	0.24	0.56	7.9	
A(4)		45	0.50	0.84	6.2	
A(34)		70	0.83	0.89	7.4	
A(25)		90	1.00	1.04	6.7	
B(21)	25.0	0	0.00	0.53	24.6	
B(32)		17	0.19	0.70	23.0	
B(4)		45	0.50	0.91	20.0	
B(34)		58	0.72	0.95	18.2	
B(25)		90	1.00	1.14	18.5	
C(21)	70.0	0	0.00	0.67	60.0	29.2
C(32)		23	0.15	0.83	57.5	30.6
C(4)		45	0.50	1.10	41.0	28.2
C(34)		74	0.90	1.10	45.0	31.8
C(25)		90	1.00	1.17	47.5	36.0

the maximum deviator stress $(\sigma_1 - \sigma_3)_{max}$, the friction angle ϕ' with respect to effective stresses, and the angle of rotation of the principal stress axes as obtained at a confining pressure of 70 lb/sq.in. are shown in Figs. 3a, 4a, and 5a respectively. It can be seen that the relationships shown in these figures are symmetrical about the 45° axis. This symmetry indicates that the samples were initially isotropic without any preferred orientation of the individual kaolinite particles, and that the test results were not affected by end restraint.

The pore-pressure coefficient A_f increased with increasing rotation of the principal stress axes (Fig. 3a). The coefficient A_f, when the principal stress axes rotated 45°, was approximately 1.40 times the pore-pressure coefficient when no rotation took place. Rotation of the principal stress axes caused a reduction of the maximum deviator stress (Fig. 4a).

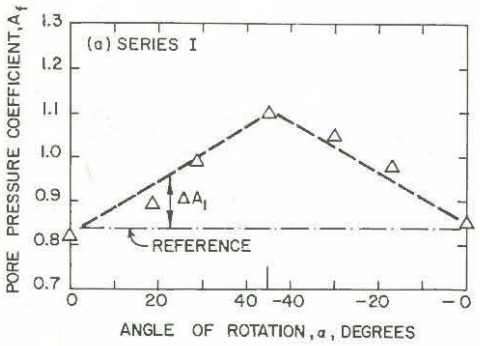

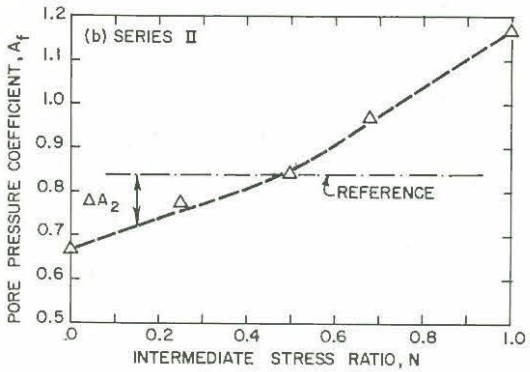

FIG. 3. Pore-pressure coefficient A_f.

An increase in rotation of 45° reduced the maximum deviator stress by one-third. It can be seen from Fig. 5a that rotation decreased the friction angle ϕ'. This friction angle decreased by 7° when the rotation of the principal stress axes increased from zero to 45°.

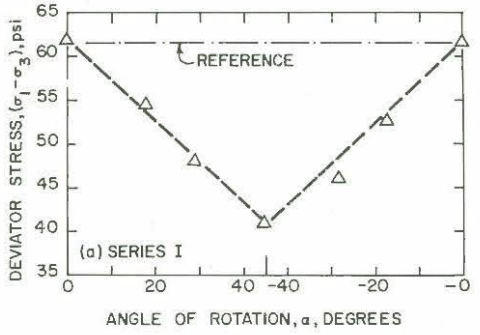

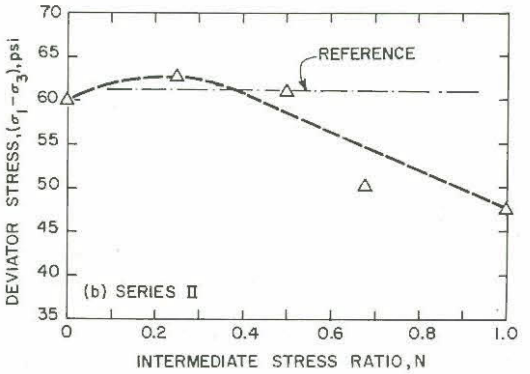

FIG. 4. Deviator stress $(\sigma_1 - \sigma_3)_{max}$.

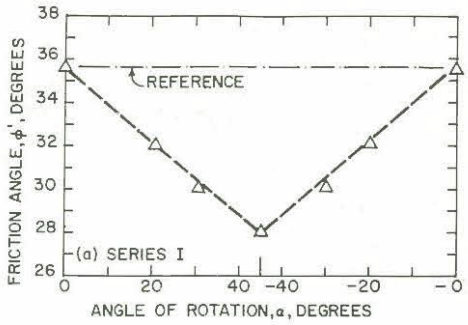

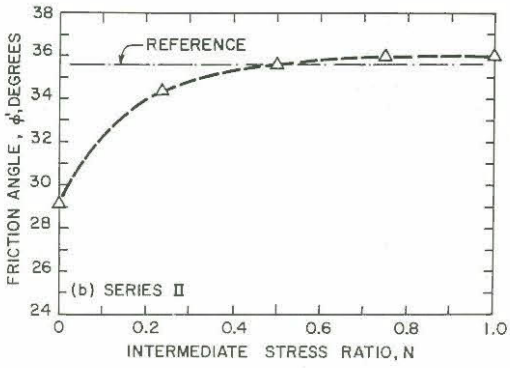

FIG. 5. Angle of internal friction ϕ'.

The effects of rotation of the principal stress axes can be attributed to the reorientation of the individual clay particles which takes place initially during the undrained phase of each test. It has been observed (Lambe, 1958; Hvorslev, 1960) that flat clay particles have a tendency to orient themselves perpendicular to the direction of the major principal stress. If, for example, the direction of the major principal stress has rotated through an angle of 45° at failure, then the orientation of the failure surface will almost coincide with the orientation of the clay particles which rotated during the initial phase of each test. The tendency of the individual clay particles to align themselves parallel with the final failure plane will increase with increasing rotation of the principal stress axes. Thus it can be expected that the maximum deviator stress and the friction angle ϕ' will decrease with increasing rotation of the principal stress axes. Such a decrease was observed. Due to the alignment of the individual clay particles and the resulting decrease of particle interlocking, it is also expected that the pore pressures at failure at a given void ratio will increase with increasing rotation of the principal stress axes.

Series II

The measured relationships between the pore-pressure coefficient A_f at failure, the maximum deviator stress $(\sigma_1 - \sigma_3)_{max}$, the angle of internal friction ϕ', and the intermediate principal stress ratio N are shown in Figs. 3b, 4b, and 5b, respectively.

It can he seen from Fig. 3b that the pore-pressure coefficient A_f increased approximately linearly with increasing stress ratio N. Fig. 4b indicates that the maximum deviator stress $(\sigma_1 - \sigma_3)_{max}$ increased with increasing N and reached maximum at $N = 0.25$. At further increases of the intermediate principal stress ratio the maximum deviator stress decreased. The maximum deviator stress obtained for the compression tests $(N = 0)$ was approximately 25 per cent

TABLE II. COMPARISON WITH TEST DATA (SERIES III)

Test no.	A_{test}	A_{calc}	$(\sigma_1 - \sigma_3)_{test}$ (psi)	$(\sigma_1 - \sigma_3)_{calc}$ (psi)	ϕ'_{test} (deg.)	ϕ'_{calc} (deg.)
Test C(32)	0.83	0.84	57.5	53.0	30.6	28.6
Test C(34)	1.10	1.20	45.0	42.5	31.8	31.7

larger than that obtained for the extension tests ($N = 1$). These results are in agreement with those reported by Taylor (1955), Henkel (1958), and Hirschfeld (1958). The friction angle ϕ' (Fig. 5b) increased rapidly with increasing intermediate principal stress ratio for values of N less than 0.25. At values of N larger than 0.25 the increase in ϕ' was small. The difference in the value of ϕ' between axial compression and axial extension tests was approximately 7°.

Series III

The combined effects of rotation of the principal stress axes and of intermediate principal stress were investigated in series III. The test data, presented in Table I, indicate that the combined effects of these two parameters can be predicted by the principal of superposition. The results obtained from tests 1 or 7 are common to both series I and II and hence can be used as reference data, as illustrated in Figs. 3, 4, and 5.

As an example, the coefficient $A(\alpha = 23°, N = 0.153)$ corresponding to $N = 0.153$ and $\alpha = 23°$ can be predicted as the reference coefficient $A(\alpha = 0, N = 0.5)$ corresponding to $N = 0.5$ and $\alpha = 0$ corrected for rotation of the principal stress axes and the intermediate principal stress ratio as expressed by the equation:

$$A(\alpha = \alpha_1, N = N_1) = A(\alpha = 0, N = 0.5) + \Delta A_1 + \Delta A_2.$$

The deviation ΔA_1 from the reference coefficient ($N = 0.5$, $\alpha = 0$) caused by a 23° rotation of the principal stress axes can be determined as shown in Fig. 3a. It is equal to the difference between the coefficient A_f corresponding to $\alpha = 23°$ and $N = 0.5$ and the reference value. Similarly the deviation ΔA_2 caused by the intermediate principal stress ratio ($N = 0.153$) can be evaluated as the difference between the coefficient A_f corresponding to $\alpha = 0$ and $N = 0.153$, and the reference value. The reference value of the coefficient A_f ($\alpha = 0$ and $N = 0.5$) is equal to 0.84. The quantities ΔA_1 and ΔA_2 determined by the proposed method are equal to 0.12 and −0.12 respectively. Hence the predicted value of A_f corresponding to $N = 0.153$ and $\alpha = 23°$ is therefore equal to 0.84. This value compares well with the measured value of 0.83 as shown in Table II. In a similar manner the maximum deviator stress and the angle of internal friction can be calculated for any rotation and for any value of the intermediate principal stress ratio. The predicted values of the pore-pressure coefficient A_f, the deviator stress, and the friction angle ϕ' agree closely with those determined experimentally from series III as shown in Table II.

The test data indicate that the principle of superposition is applicable and that the shear-strength and pore-pressure parameters can be predicted for any value of rotation of the principal stress axes and for any value of the intermediate principal stress ratio from two series of tests where the effects of these two parameters have been evaluated separately.

ACKNOWLEDGMENT

This study was sponsored by the National Science Foundation (Grant NSF-G21833).

REFERENCES

CASBARIAN, A. O. (1964). Effects of rotation of the principal stress axes and of the intermediate principal stress on the shear strength of a saturated remolded clay. Ph.D. thesis, Cornell University, Ithaca, New York.

HABIB, P. (1953). Influence de la variation de la contrainte principale moyenne sur la résistance au cisaillement des sols. *Proc. Third International Conference on Soil Mechanics and Foundation Engineering*, Vol. 1, pp. 131–6.

HENKEL, D. J. (1958). The correlation between deformation, pore water pressure and strength characteristics of saturated clays. Ph.D. thesis, University of London, England.

HIRSCHFELD, R. C. (1958). Factors influencing the constant volume strength of clays. Sc.D. thesis, Harvard University, Cambridge, Massachusetts, 398 pp.

HVORSLEV, M. J. (1960). Physical components of the shear strength of saturated clays. *Proc. Research Conference on Shear Strength of Cohesive Soils* (Boulder, Colorado), pp. 169–273.

LAMBE, T. W. (1958). The structure of compacted clay. *Proc. American Society of Civil Engineers*, Vol. 84, No. SM2, Paper 1654.

RENDULIC, L. (1936). Relation between void ratio and effective principal stresses for a remolded silty clay. *Proc. First International Conference on Soil Mechanics and Foundation Engineering*, Vol. 3, pp. 48–51.

TAYLOR, D. W. (1955). Review of research on shearing resistance of clay. Report submitted to the United States Army Engineers Waterways Experimental Station.

WU, T. H., A. K. LOH, and L. E. MALVERN (1963). Study of failure envelope of soils. *Proc. American Society of Civil Engineers*, Vol. 89, No. SM1, pp. 145–81.

Analysis of the Triaxial Test—Cohesionless Soils

Analyse de l'essai triaxial—sols pulvérulents

B. B. BROMS, PH.D., *Associate Professor of Civil Engineering, Cornell University, Ithaca, U.S.A.*
A. K. JAMAL, B.SC.(Dunelm), M.S., *Aggrey Fellow, Cornell University, Ithaca, U.S.A.*

SUMMARY

Solid and hollow samples of a cohesionless soil have been tested to failure under undrained conditions. For some of the hollow specimens, volume changes of the inside chamber were prevented. By measuring the inside chamber pressure, it has been possible to measure directly the corresponding radial stress in a solid sample.

The test data indicate that for cohesionless soils the standard triaxial test will underestimate the angle of internal friction ϕ' by approximately 3 to 4 degrees when the relative density is high while at medium to low relative densities, the friction angle ϕ' determined from standard triaxial tests will correspond to its maximum possible value. A difference in the friction angle ϕ' of 3 to 4 degrees is sufficient to explain the difference observed by a number of investigators for dense sand between extension and compression tests and between the calculated and measured bearing capacity of model footings.

SOMMAIRE

Des échantillons creux et pleins d'un sol sans cohésion ont été examinés dans des conditions non-drainées. Pour une partie des échantillons creux, les changements de volume de la chambre intérieure furent empêchés. En mesurant la pression de la chambre intérieure il fut possible de mesurer directement la contrainte radiale correspondante dans un échantillon plein.

Les résultats des épreuves indiquent que pour des sols sans cohésion les essais triaxiaux sous-estiment l'angle de friction interne ϕ' d'environ 3 à 4 degrés quand la densité relative est forte; pour des densités intermédiaires et faibles, l'angle de friction ϕ' déterminé par des essais triaxiaux correspond à sa valeur maximale. Une différence de 3 à 4 degrés dans l'angle de friction est suffisante pour expliquer la différence observée par plusieurs chercheurs dans le cas d'un sable dense entre des épreuves de tension et de compression et entre la force portante calculée et mesurée pour les semelles modèles.

IN THE ANALYSIS of the standard triaxial compression test, it is generally assumed that the stresses within the soil specimen are uniformly distributed and that the intermediate principal stress is equal to the minor principal stress. The test results are usually analysed by the Coulomb-Mohr failure criterion and the shear strength of the soil is expressed in terms of an angle of internal friction ϕ and a cohesion c.

For cohesionless soils the angle of internal friction ϕ' with respect to effective stresses as measured by axial compression tests has been found by several investigators to be lower than that measured by axial extension tests (Taylor, 1941; Habib, 1953; Peltier, 1957; Henkel, 1959; Haythornthwaite 1960) or that measured under the condition of plane strain (Bishop, 1961; Whitman and Luscher, 1962). On the other hand, Bishop and Eldin (1953) and Kirkpatrick (1957) have found close agreement between compression and extension tests.

Experiments by Hansen (1961) and by Tcheng (1957) have indicated that the bearing capacity of model footings placed on dense sand may exceed considerably that predicted by existing bearing capacity theories if the shear-strength parameters determined from standard triaxial compression tests are used in the analysis of the test data. However, close agreement was found for footings located on medium to loose sand.

The observed differences between compression and extension tests and between compression tests and tests carried out under the condition of plane strain can be attributed to a non-uniform stress distribution within the standard triaxial test specimen as will be shown by the investigation described in this paper. This non-uniform stress distribution can also explain the observed differences between measured and calculated bearing capacity which have been observed for model footings placed on dense sand.

STRESS DISTRIBUTION WITHIN TRIAXIAL TEST SPECIMEN

In a standard triaxial compression test, the major principal stress, σ_z, acts in the direction of the axis of the test specimen. Its average value, $(\sigma_z)_{av}$ is equal to P/A where P is the applied axial load and A is the cross-sectional area. The radial stress, σ_r, and the circumferential stress, σ , (defined in Fig. 1) may be either the intermediate or the minor

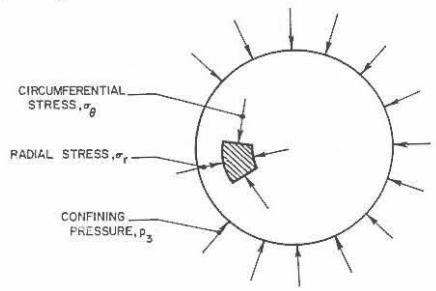

FIG. 1. Circumferential and radial stresses.

principal stress. The stress distribution when the radial stress increases toward the centre of the test specimen is shown in Fig. 2a and the stress distribution when the radial stress decreases toward the centre is shown in Fig. 2b.

The average circumferential stress $(\sigma_\theta)_{av}$ can be calculated from equilibrium conditions and is equal to the applied confining pressure, p_3. The radial stress, σ_r, is equal to the confining pressure p_3 at the surface of the test member specimen (Fig. 2). For the case (case I) when the radial stress increases toward the centre of the test specimen, the average radial stress $(\sigma_r)_{av}$ will be larger than the confining pressure p_3; while for the case (case II) when the radial stress decreases toward the centre, its average value will be less than the confining pressure p_3.

Reprinted from *Proc. 6th internat. Conf. Soil Mech., 1965.* Printed in Canada.

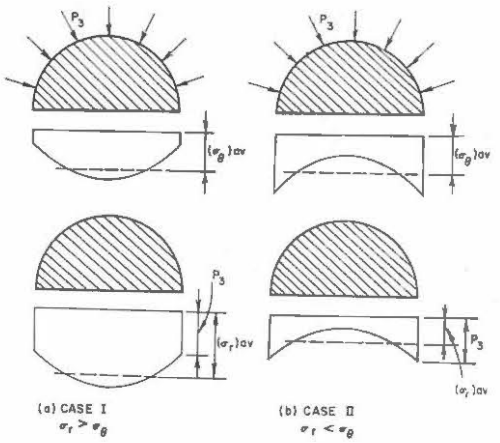

FIG. 2. Stress distribution.

Mohr's stress circles corresponding to the two cases are shown in Fig. 3. The shear-strength parameters ϕ and c are generally determined by constructing the envelope curve to a series of stress circles governed by the average axial stress (P/A) at failure and the confining pressure p_3. For case I, the shear strength parameters ϕ and c will be equal to ϕ_a and c_a, whereas for case II, these parameters will be equal to ϕ_b and c_b. The friction angle ϕ_b and the cohesion c_b, corresponding to the major and the intermediate principal stresses, may be considerably smaller than the shear-strength parameters ϕ_a and c_a corresponding to the major and minor principal stresses.

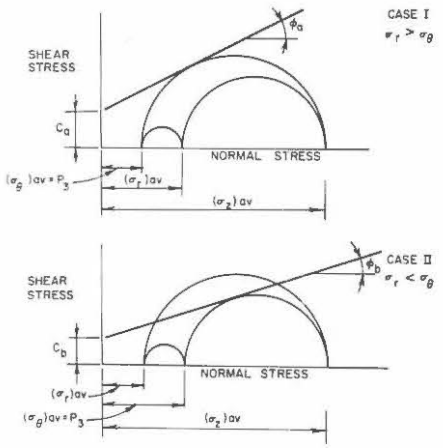

FIG. 3. Interpretation of triaxial tests.

In the case when the radial stress decreases towards the centre, the angle of internal friction will correspond to the major and the intermediate principal stresses rather than the major and minor principal stresses. For this case, the standard triaxial test will underestimate the angle of internal friction.

OUTLINE OF TEST PROGRAMME

In a standard triaxial test specimen, all radial planes are planes of symmetry and the shear stresses on these planes will at all times be equal to zero. Since the shear stresses on two perpendicular planes are always equal, the shear stress on any circumferential plane will be equal to zero, the latter being perpendicular to the radial planes. Therefore, the shear stress will be equal to zero on the plane corresponding to the inside surface of a hollow cylindrical specimen with the same outside dimensions as those of the corresponding solid specimen. The centre core of a solid specimen may therefore be replaced by a liquid and in this case, the shear stress along the inside face of the resulting hollow specimen will also be equal to zero.

Furthermore, the liquid will have the same deformation characteristics (it is incompressible) as the saturated soil it replaces if volume changes are prevented in the hollow specimen. Thus, by measuring the changes in the inside chamber pressure for the hollow specimen, the corresponding changes in the radial stress can be measured directly for the standard solid triaxial specimen.

In order to investigate the hypothesis presented above, three series of consolidated-undrained tests were carried out on a beach sand at different relative densities. In series I, solid samples with a diameter of 3.0 in. and a height of 6.0 in. were tested while in series II and III, hollow cylindrical samples with a height of 12.0 in. and with outside and inside diameters of 6.0 and 3.0 in., respectively, were tested. The inside chamber pressure was kept constant in series II. In this series, volume changes of the inside chamber were allowed. The volume of the inside chamber was kept constant in series III and the resulting changes of the inside chamber pressure were measured. All tests were carried out at a constant axial strain rate of 0.1 per cent per minute.

MATERIAL AND TEST APPARATUS

A beach sand consisting of rounded quartz particles of a high degree of purity was used in this investigation. The grain size ranged from 0.8 mm to 0.1 mm. The coefficient of uniformity of the sand was 1.67 and its effective grain size was 0.18 mm. The specific gravity of the quartz particles was 2.65 and the maximum and minimum porosities of the sand were 0.50 and 0.36, respectively (Kolbuszewski, 1948).

A standard cell was used for the solid specimens tested in series I. A modified triaxial cell was utilized for series II and III. The hollow cylindrical test specimen was sealed between an inner and an outer rubber membrane and between two ring plates. Pressure changes in the inside chamber of the hollow specimens (series III) were measured by a simple differential mercury manometer, volume changes being prevented by means of a null indicator and a back pressure system.

TEST PROCEDURE

The sand used in this investigation was boiled before moulding in order to ensure a maximum degree of saturation. Different compaction procedures were used to vary the relative density of the sand. To obtain a medium to low relative density (Meyerhof, 1956), the sand was placed under water in three layers and each layer was rodded lightly. For a relative density ranging from medium to dense, the sand was placed under water and vibrated for 5, 15, or 30 seconds on a vibrating table. By such a procedure, the porosity could be varied between 0.36 and 0.44 for the solid samples and between 0.38 and 0.46 for the thin-walled hollow samples.

The specimens were allowed to consolidate fully at a confining pressure of 7.1 or 14.2 lh/sq. in. whereafter a back pressure was applied to ensure full saturation. By increasing the confining pressure slightly and by measuring the resulting pore-pressure increase, the degree of saturation of the test specimens could be checked. The test specimens were then tested to failure under undrained conditions and under increasing axial load. The resulting pore-pressure changes were measured.

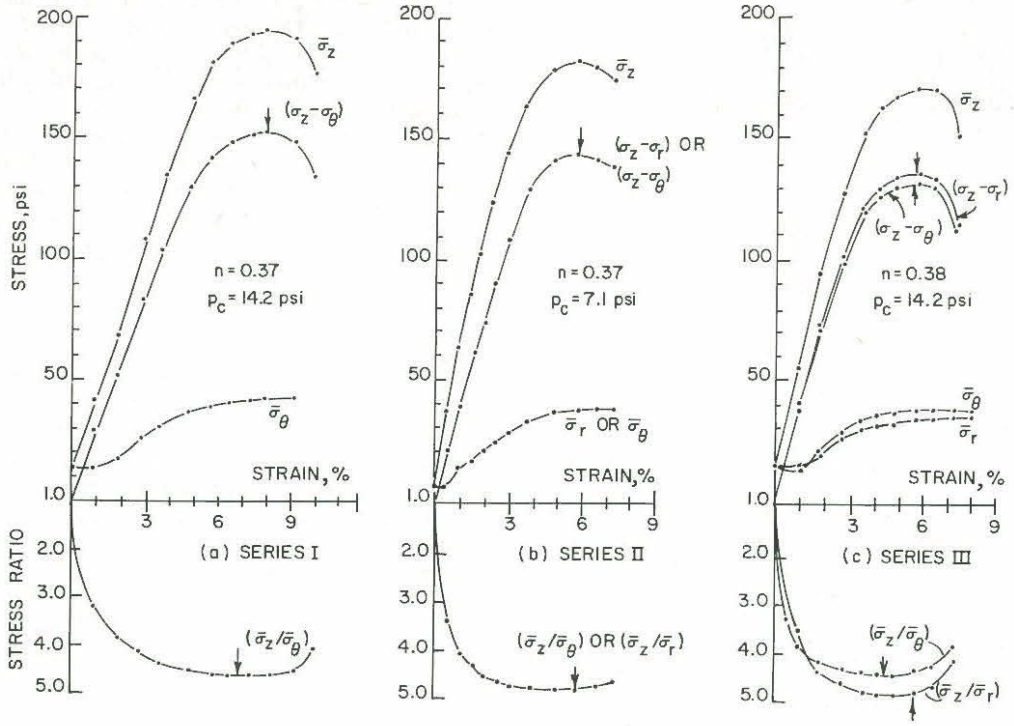

FIG. 4. Typical stress-strain relationships—high relative density.

TEST RESULTS

Stress-Strain Relationships

Typical stress-strain relationships as obtained from the solid samples (series I), the hollow samples where volume changes of the inside chamber were allowed (series II), and the hollow samples where no volume changes of the inside chamber were allowed (series III) are shown in Figs. 4 and 5. The relationships shown in Fig. 4 are those for specimens at a high relative density (corresponding low porosity) while those shown in Fig. 5 were obtained for specimens having medium to low relative density (medium to high porosity).

For the solid specimens, the maximum principal stress ratio $(\bar{\sigma}_z/\bar{\sigma}_\theta)_{max}$ was reached at an axial strain which was smaller than that corresponding to the maximum deviator stress $(\sigma_z - \sigma_\theta)$ as shown in Fig. 4a, while for the solid samples with a medium relative density, the strains corresponding to $\bar{\sigma}_z/\bar{\sigma}_\theta)_{max}$ and to $(\sigma_z - \sigma_\theta)_{max}$ were approximately the same (Fig. 5a). The strains corresponding to $\bar{\sigma}_z/\bar{\sigma}_r)_{max}$ or $(\sigma_z - \sigma_r)_{max}$ were, as shown in Figs. 4b and 5b, approximately the same for the hollow samples where volume changes of the inside chamber were allowed (series II) regardless of the initial porosity of soil.

For the hollow samples at high relative density where volume changes of the inside chamber were prevented

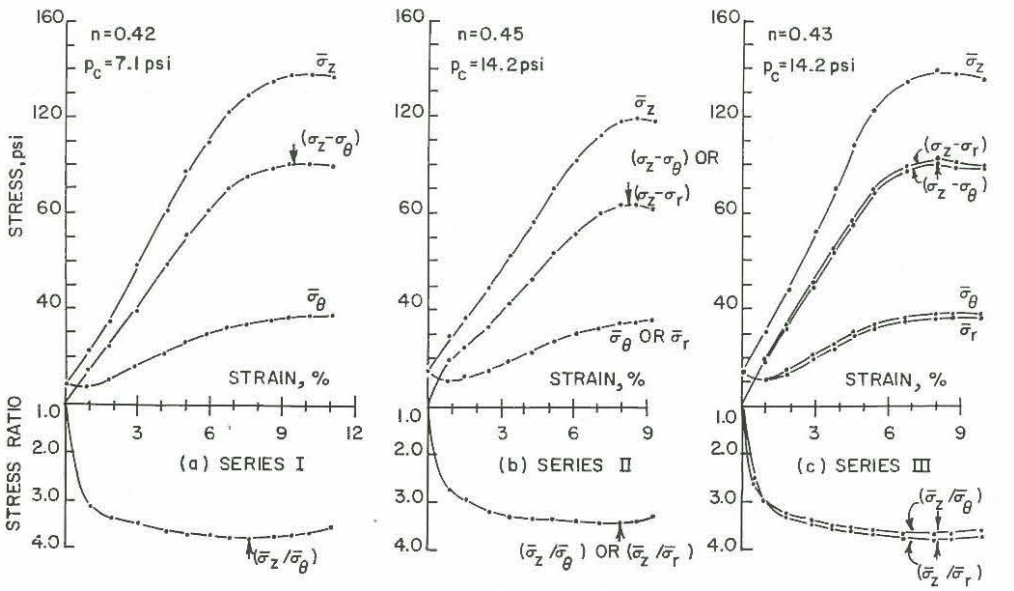

FIG. 5. Typical stress-strain relationships—low relative density.

(series III), the maximum principal stress ratio $(\bar{\sigma}_z/\bar{\sigma}_\theta)_{max}$ with respect to the average effective circumferential stress was reached at a strain less than that corresponding to the maximum deviator stress $(\sigma_z - \sigma_\theta)_{max}$. The strain corresponding to $(\sigma_z/\sigma_\theta)_{max}$ was approximately equal to that measured for the solid samples (Fig. 4a).

It can be seen from Fig. 4c that for series III, the strain corresponding to $(\bar{\sigma}_z/\bar{\sigma}_r)_{max}$ is approximately equal to that corresponding to $(\sigma_z - \sigma_r)_{max}$. This strain is approximately equal to that corresponding to $(\bar{\sigma}_z/\bar{\sigma}_r)_{max}$ as obtained for the hollow samples tested in series II (Fig. 4b). For the samples with a medium to low relative density in series III (Fig. 5c), the strains corresponding to $(\bar{\sigma}_z/\bar{\sigma}_\theta)_{max}$ and to $(\bar{\sigma}_z/\bar{\sigma}_r)_{max}$ are approximately the same. These strains compare well with those measured for series I and II (Figs. 5a and 5b).

From the stress-strain relationships in Figs. 4c and 5c (series III), it can be noted that the circumferential effective stress $(\bar{\sigma}_\theta)_{av}$ is smaller than the radial stress $(\bar{\sigma}_r)_{av}$ at axial unit deformation less than about 2 per cent, while at larger deformations, the circumferential stress is larger than the radial stress. Thus, the circumferential stress is the minor principal stress at small axial deformations while at relatively large axial deformations, the radial stress is the minor principal stress.

Friction Angle ϕ'

For series III (Fig. 4c), the ratio $(\bar{\sigma}_z/\bar{\sigma}_\theta)_{max}$ is smaller than the ratio $(\bar{\sigma}_z/\bar{\sigma}_r)_{max}$, thus indicating that for dense sand, the friction angle ϕ' corresponding to the axial and the radial stresses is larger than that corresponding to the axial and the circumferential stresses. For the hollow specimens tested at low relative density (Fig. 5c) the difference between the stress ratios $(\bar{\sigma}_z/\bar{\sigma}_\theta)_{max}$ and $(\bar{\sigma}_z/\bar{\sigma}_r)_{max}$ is small and the maximum values of these stress ratios occurred approximately at the same axial unit deformation. Thus, for this case, the friction angle ϕ' corresponding to the axial and the circumferential stresses is approximately equal to that corresponding to the axial and the radial stresses.

The shape of the stress-strain relationships and differences between the $(\bar{\sigma}_z/\bar{\sigma}_\theta)_{max}$ and $(\bar{\sigma}_z/\bar{\sigma}_r)_{max}$ observed for series III indicate that the standard triaxial test tends to underestimate the shear-strength parameter ϕ' at high relative densities of the cohesionless soils, while at medium or low relative densities, the standard triaxial test will give a true indication of this shear-strength parameter.

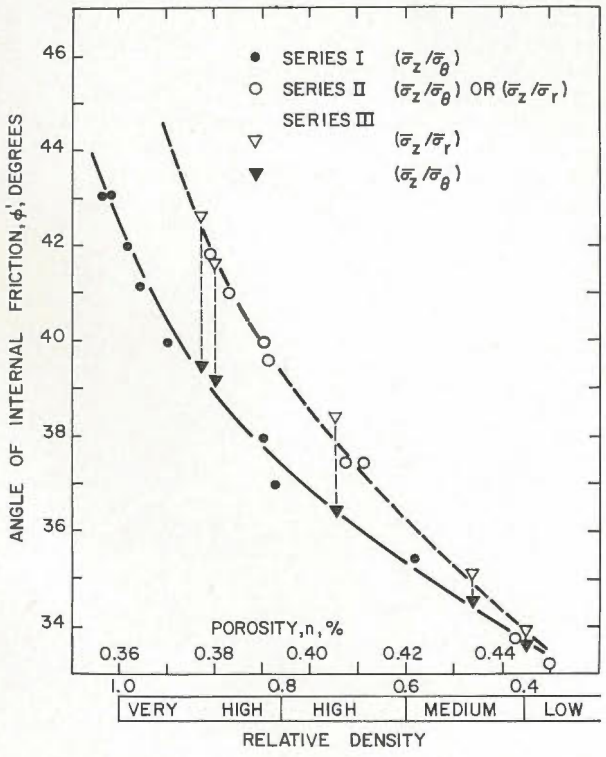

FIG. 6. Relationships between friction angle ϕ' and porosity.

Relationship between Porosity and Friction Angle ϕ'

Since the porosity varied slightly between the individual tests and between the hollow and the solid specimens, a direct comparison between series I, II, and III cannot be made. In order to correct for differences in porosity, the calculated friction angle ϕ' corresponding to either $(\bar{\sigma}_z/\sigma_r)_{max}$ or to $(\bar{\sigma}_z/\bar{\sigma}_\theta)_{max}$ has been plotted in Fig. 6 as a function of the initial porosity of the samples.

It can be seen that the friction angle ϕ' corresponding to $(\bar{\sigma}_z/\bar{\sigma}_\theta)_{max}$ determined from series III is approximately equal to that determined from the standard trixial test specimen (the solid samples) and that the friction angle ϕ' at $(\bar{\sigma}_z/\bar{\sigma}_r)_{max}$ corresponds closely to that determined from series II. The difference between the two values of the friction angle ϕ' is about 3 to 4 degrees at a high relative density, and this difference decreases with decreasing relative density (increasing porosity). The difference is relatively small at medium and low relative densities.

A difference of 3 to 4 degrees in the friction angle ϕ' is sufficient to account for the differences observed between the extension and compression tests and for the difference observed between measured and calculated bearing capacity of model footings.

ACKNOWLEDGMENT

This investigation has been supported by the National Science Foundation (Grant No. G-21833).

REFERENCES

BISHOP, A. W. (1961). Discussion, Section I. *Proc. Fifth International Conference on Soil Mechanics and Foundation Engineering*, Vol. 3, pp. 97–100.

BISHOP, A. W., and A. K. G. ELDIN (1953). The effect of stress history on the relation between ϕ and porosity in sand. *Proc. Third International Conference on Soil Mechanics and Foundation Engineering*, Vol. 1, pp. 100–5.

HABIB, P. (1953) Influence de la variation de la contrainte principale moyenne sur la résistance au cisaillement des sols. *Proc. Third International Conference on Soil Mechanics and Foundation Engineering*, Vol. 1, pp. 131–6.

HANSEN, B. (1961). The bearing capacity of sand, tested by loading circular plates. *Proc. Fifth International Conference on Soil Mechanics and Foundation Engineering*, Vol. 1, pp. 659–64.

HAYTHORNTHWAITE, R. M. (1960). Mechanics of the triaxial test for soils. *Proc. American Society of Civil Engineers*, Vol. 86, No. SM5, Paper 2625, pp. 35–62.

HENKEL, D. J. (1959). The relationships between the strength, pore water pressure and volume change characteristics of saturated clays. *Géotechnique*, Vol. 9, pp. 119–35.

KIRKPATRICK, W. M. (1957). The condition of failure for sands, *Proc. Fourth International Conference on Soil Mechanics and Foundation Engineering*, Vol. 1, pp. 172–8.

KOLBUSZEWSKI, J. J. (1948). An experimental study of the

maximum and minimum porosities of sands. *Proc. Second International Conference on Soil Mechanics and Foundation Engineering*, Vol. 1, pp. 158–65.

MEYERHOF, G. G. (1956). Penetration tests and bearing capacity of cohesionless soils. *Proc. American Society of Civil Engineers*, Vol. 82, No. SM1, Paper 866, pp. 1–19.

PELTIER, M. R. (1957). Experimental investigations of the intrinsic rupture curve of cohesionless soils. *Proc. Fourth International Conference on Soil Mechanics and Foundation Engineering*. Vol. 1, pp. 179–82.

TAYLOR, D. W. (1941). Seventh Progress Report on Shear Research to U.S. Corps of Engineers. MIT Publication, Cambridge, Mass.

TCHENG, Y. (1957). Fondations superficielles en milieu stratifié. *Proc. Fourth International Conference on Soil Mechanics and Foundation Engineering*, Vol. 1, pp. 449–52.

WHITMAN, R. V. and U. LUSCHER (1962). Basic experiment into soil-structure interaction. *Proc. American Society of Civil Engineers*, Vol. 88, No. SM6, pp. 135–67.